

E_1/E_2 traps in 6H-SiC studied with Laplace deep level transient spectroscopy

A. Koizumi,^{1,2,a),b)} V. P. Markevich,² N. Iwamoto,³ S. Sasaki,⁴ T. Ohshima,³ K. Kojima,⁵ T. Kimoto,⁴ K. Uchida,¹ S. Nozaki,¹ B. Hamilton,² and A. R. Peaker²

¹Department of Electronic Engineering, University of Electro-Communications, 1-5-1 Chofugaoka, Chofu, Tokyo 182-8585, Japan

²School of Electrical and Electronic Engineering, University of Manchester, Manchester M13 9PL, United Kingdom

³Semiconductor Analysis and Radiation Effects Group, Japan Atomic Energy Agency, 1233 Watanuki, Takasaki, Gunma 370-1292, Japan

⁴Department of Electronic Science and Engineering, Kyoto University, Katsura, Nishikyo, Kyoto 615-8510, Japan

⁵Advanced Power Electronics Research Center, National Institute of Advanced Industrial Science and Technology, 1-1-1 Umezono, Tsukuba, Ibaraki 305-8568, Japan

(Received 30 October 2012; accepted 8 January 2013; published online 23 January 2013)

Electrically active defects in *n*-type 6H-SiC diode structures have been studied by deep level transient spectroscopy (DLTS) and high-resolution Laplace DLTS. It is shown that the commonly observed broadened DLTS peak previously ascribed to two traps referenced as E_1/E_2 has three components with activation energies for electron emission of 0.39, 0.43, and 0.44 eV. Further, defects associated with these emission signals have similar electronic structure, each possessing two energy levels with negative-*U* ordering in the upper half of the 6H-SiC gap. It is argued that the defects are related to a carbon vacancy at three non-equivalent lattice sites in 6H-SiC. © 2013 American Institute of Physics. [<http://dx.doi.org/10.1063/1.4788814>]

Silicon carbide (SiC) is one of the wide-bandgap semiconductors which appear promising for realizing high-power and high-temperature electronic devices.¹ In addition, SiC diodes can be used as high-energy particle detectors and have some advantages over silicon detectors because of a wider bandgap of SiC.² In these applications, the presence of various defects affects device performance due to carrier trapping, increased leakage current, and reduced minority carrier lifetime. This letter describes the use of high resolution Laplace deep level transient spectroscopy (LDLTS) as a tool to characterize the behavior of some ubiquitous electrically active defects in SiC.

A signal due to the so called E_1/E_2 electron traps has been commonly observed by deep level transient spectroscopy (DLTS) in p^+n diode structures fabricated in *n*-type 6H-SiC.^{3–5} It is well established that the magnitude of the E_1/E_2 DLTS peak is increased by both ion implantation and electron irradiation.^{3–10} The peak also has a shoulder indicating that it is not a single point defect. Previously, the peak has been separated into two components, and the corresponding activation energies for electron emission determined by fitting the DLTS spectra calculated using a two-trap model or by employing the three-point-correlation window DLTS method,¹¹ which has an improved energy resolution in comparison with conventional DLTS.^{6,12} The E_1 and E_2 deep levels were attributed to defects with a similar structure, which reside on different lattice sites.³ This attribution was, however, questioned by Pensl *et al.*⁹ In 6H-SiC there are

three non-equivalent lattice sites for the vacancy, one with hexagonal (*h*) and the other two with cubic (k_1 and k_2) symmetry.¹³ The difference in the local structure of the lattice can cause a small difference in energy levels of an electrically active defect, which resides on different lattice sites.¹⁴ The separation of the E_1/E_2 DLTS peak into two components is not consistent with a three level structure expected for an electrically active simple defect residing on different lattice sites in 6H-SiC. It might be possible, however, that the separation of the E_1/E_2 DLTS signal into only two components is related to the insufficient resolution of the conventional DLTS technique.

In this letter, we show that the E_1/E_2 DLTS peak in 6H-SiC can be successfully resolved into three components using high resolution LDLTS.¹⁵ Furthermore, it has been found that defects associated with these components are of the same fundamental electronic structure, each having two energy levels with negative-*U* ordering in the upper half of the gap.

For these experiments, we used two kinds of 6H-SiC diode samples, p^+n diodes¹⁶ and *n*-type Schottky barrier diodes (SBDs).⁵ The p^+n diodes were fabricated on *n*-type epi-layer grown on *n*-type 6H-SiC substrate {CREE, 3.5° off-axis (0001)} by hot-wall chemical vapor deposition. The net donor concentration in the epi-layer and its thickness were approximately $2 \times 10^{15} \text{ cm}^{-3}$ and 4 μm , respectively. The 150 nm-thick p^+ layer ($N_A = 5 \times 10^{19} \text{ cm}^{-3}$) of the diode was formed by implantation of aluminum ions at 800 °C, followed by a post-implantation annealing at 1800 °C for 10 min in an argon ambient. Sequential ion implantations of aluminum were carried out with energies of 110, 75, and 50 keV for doses of 4.2×10^{14} , 1.3×10^{14} , and $1.2 \times 10^{14} \text{ cm}^{-2}$, respectively, to form a nearly uniform aluminum depth profile within 150 nm.¹⁶ A top Ohmic contact to the p^+ region was

^{a)}Author to whom correspondence should be addressed. Electronic mail: koizumi@mat.eng.osaka-u.ac.jp.

^{b)}Present address: Division of Materials and Manufacturing Science, Graduate School of Engineering, Osaka University, 2-1 Yamadaoka, Suita, Osaka 565-0871, Japan.

formed by aluminum deposition and subsequent sintering at 850 °C for 5 min. A bonding pad on the sintered aluminum layer and a bottom Ohmic contact were made by aluminum deposition without sintering. For comparison with the p^+n diodes, the n -type SBDs were fabricated on an n -type epi-layer grown on a 3.5° off-axis 6H-SiC (0001) substrate.¹⁷ The doping concentration in the epi-layer was $5 \times 10^{15} \text{ cm}^{-3}$. Electron irradiation of the SBD structures was performed at an energy of 150 keV and fluences of 1×10^{16} and $4 \times 10^{17} \text{ cm}^{-2}$ without intentional heating. This low-energy e^- -irradiation results in the selective displacement of carbon atoms in SiC crystals.^{10,18,19} After the e^- -irradiation, the samples were annealed in an argon ambient at 950 °C for 30 min. In the conventional DLTS and LDLTS measurements, we typically used the reverse bias $V_r = -7 \text{ V}$, pulse voltage $V_p = 0 \text{ V}$, and filling pulse width $t_p = 1 \text{ ms}$.

Figure 1 shows a conventional DLTS spectrum for an unirradiated p^+n diode and two spectra for electron-irradiated SBD samples. The SBD samples were irradiated with electron fluences of 1×10^{16} and $4 \times 10^{17} \text{ cm}^{-2}$. The spectra were recorded with a rate window of 80 s^{-1} . A complex DLTS peak labeled E_1/E_2 is observed in all the spectra. For the SBD structures, the E_1/E_2 peak intensity is much stronger in the sample which was irradiated with higher fluence of 150 keV electrons. An analysis of the DLTS spectrum of the p^+n diode shows a high concentration of the defects associated with the E_1/E_2 peak even though the p^+n diode was not irradiated with electrons. In the analysis, N_T/N_d was found to be close to 0.3, where N_T is the total concentration of the defects responsible for the E_1/E_2 peak, and N_d is the net shallow donor concentration. Uedono *et al.* reported implantation-induced vacancy-related defects observed at depths significantly deeper than the mean ion projected range R_p .^{20,21} In our p^+n diodes, the net donor concentration estimated from the capacitance-voltage characteristic at room temperature decreases from about $2.3 \times 10^{15} \text{ cm}^{-3}$ at the end of the depleted region ($W \cong 2.44 \mu\text{m}$ at $V_r = -7 \text{ V}$) to about $1.6 \times 10^{15} \text{ cm}^{-3}$ at the depletion width for $V_p = 0 \text{ V}$ ($W \cong 1.45 \mu\text{m}$). Considering the position of the Fermi level (E_F is at about $E_c - 0.275 \text{ eV}$ at

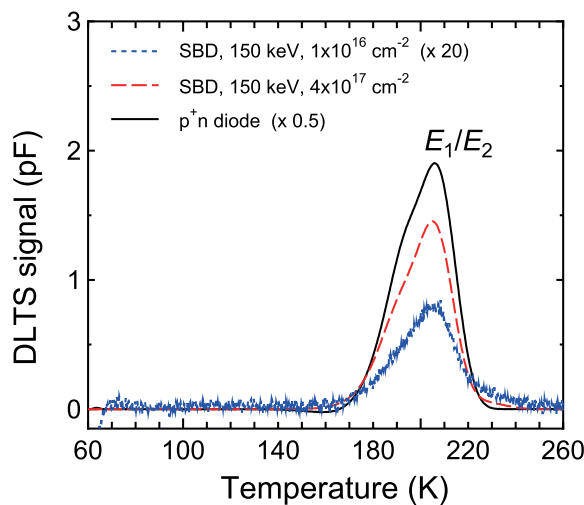


FIG. 1. Conventional DLTS spectra for unirradiated 6H-SiC p^+n diode (solid line) and n -type 6H-SiC SBD sample irradiated with 150 keV electrons with fluences of $1 \times 10^{16} \text{ cm}^{-2}$ (short-dashed line) and $4 \times 10^{17} \text{ cm}^{-2}$ (dashed line). A rate window of 80 s^{-1} was used in the measurements.

300 K in these diodes) and electronic properties of the E_1/E_2 traps, which will be discussed in detail in the following, the observed decrease in the net donor concentration is associated with the increased concentration of the acceptor-like E_1/E_2 traps, which are partially filled with electrons at 300 K, in the vicinity of the p^+n junction. Furthermore, in agreement with Uedono *et al.* results,^{20,21} it is also suggested that the E_1/E_2 traps were introduced into the n region near the p^+n junction by aluminum implantation.

Figure 2 shows the LDLTS spectra of the p^+n diode sample measured at various temperatures range from 200 to 220 K. This is the same diode whose DLTS spectrum is shown in Fig. 1. The LDLTS temperature range includes the peak temperature of the DLTS signal due to the E_1/E_2 traps in the conventional DLTS spectra (Fig. 1). In Fig. 2, the LDLTS spectra at each temperature clearly show that the DLTS signal associated with the E_1/E_2 traps consists of three emission components. An analysis of the LDLTS spectra further indicates that the DLTS signal previously attributed to the E_2 trap consists of two components with very close emission rates, which are labeled here as E_{2L} and E_{2H} . It has been mentioned above that the E_1/E_2 traps have been attributed to the same defect residing on different lattice sites in 6H-SiC.³ Our LDLTS results provide a clear confirmation of such an attribution. Furthermore, it appears that the three emission components of the E_1/E_2 DLTS signal observed for the first time by LDLTS could be related to a simple lattice defect distributed over the hexagonal (the E_1 trap) and two cubic sites (the E_{2L} and E_{2H} traps) in the 6H-SiC lattice. The Arrhenius plots for these three traps for the un-irradiated p^+n diode and e^- -irradiated SBD (with the $4 \times 10^{17} \text{ cm}^{-2}$ electron fluence) are shown in Fig. 3. The activation energies for

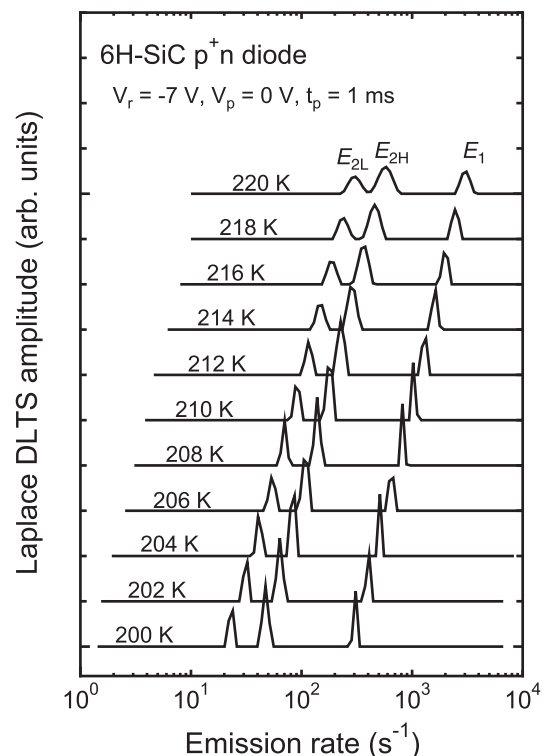


FIG. 2. LDLTS spectra of a 6H-SiC p^+n diode measured in the temperature range of 200–220 K. Measurement conditions are given in the figure.

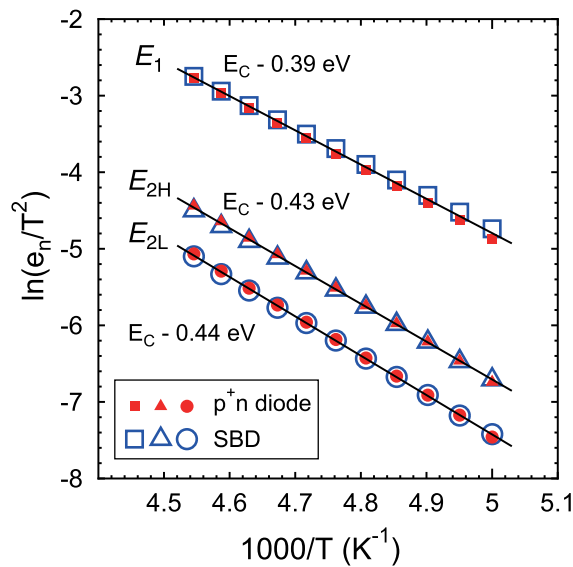


FIG. 3. Arrhenius plots of electron emission rates for the three components E_1 , E_{2H} , and E_{2L} of E_1/E_2 traps in 6H-SiC obtained by LDLTS measurements of an unirradiated p^+n diode and an electron-irradiated SBD (fluence of irradiation was $4 \times 10^{17} \text{ cm}^{-2}$).

electron emission from the E_1 , E_{2H} , and E_{2L} traps are determined to be 0.39 eV, 0.43 eV, and 0.44 eV from the conduction band edge, respectively, independent of whether the measurements were taken on the p^+n diodes or Schottky diodes.

Hemmingsson *et al.* presented some strong arguments that both the E_1 and E_2 traps had negative- U properties.²² They correlated electron emission signals due to the E_1 and E_2 traps [$E_1(-/+)$ and $E_2(-/+)$ transitions] with electron emission signals in the temperature range of 100–130 K from two shallower levels [$E_1(0/+)$ and $E_2(0/+)$ transitions]. The DLTS spectra showing the peaks from the shallower levels were recorded with a filling pulse width of 300 ns and illumination before the filling pulse to prevent the transformation from the metastable shallow level configurations to the stable deep level configurations upon capturing two electrons during application of the DLTS filling pulses. Negative- U properties of the E_1 and E_2 traps in 6H-SiC were confirmed later by Pensl *et al.*⁹

In order to evidence the negative- U properties of the E_1/E_2 traps and to obtain additional information on the electronic structure of the corresponding defects in the shallow level configuration, we have carried out some specific DLTS and LDLTS measurement procedures. In order to “freeze” the defects responsible for the E_1 , E_{2H} , and E_{2L} traps into the shallow level configuration and hence observe the emission signals from the shallower levels, we cooled down the diodes from room temperature to 50 K with a reverse bias of -7 V and then recorded the DLTS spectra during heating the samples and applying fill pulses of $1 \mu\text{s}$ width. The DLTS spectra recorded under the above conditions are presented in Fig. 4. In contrast to the DLTS spectra shown in Fig. 1, there are two small peaks at temperatures lower than 150 K besides the main E_1/E_2 related peak with the maximum at about 200 K in Fig. 4. Apparently, the use of the above measurement conditions prevented the defects responsible for E_1 , E_{2H} , and E_{2L} traps from capturing two electrons during the

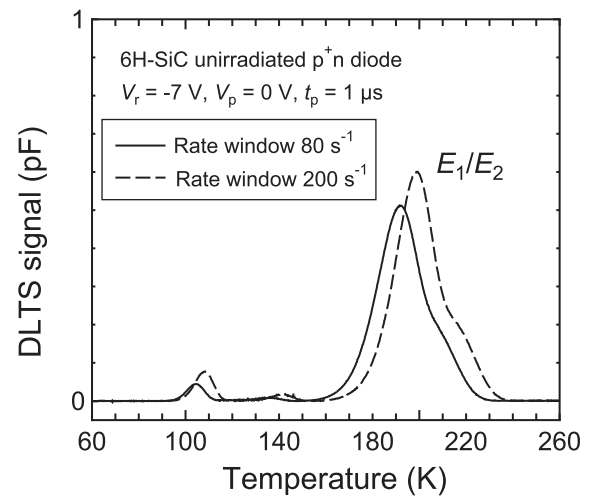


FIG. 4. Conventional DLTS spectra for an unirradiated 6H-SiC p^+n diode. The spectra were recorded with a filling pulse width of $1 \mu\text{s}$ after cooling the diode down with reverse bias of -7 V .

filling stage in the temperature range 100–150 K, transforming them into a stable configuration with deeper energy levels. Therefore, the detection of the signals due to electron emission from the metastable shallower level configuration became clearly observable. In order to resolve the emission signals from the shallower levels, LDLTS measurements were carried out on the p^+n diode in the temperature ranges of 95–105 and 130–140 K with the use of short filling pulses. Figure 5 shows the LDLTS spectra at 100 and 135 K. Two emission signals occur in the spectrum recorded at 100 K and one signal in the spectrum taken at 135 K. The two emission signals in the LDLTS spectra recorded in the temperature range of 95–105 K can be associated with the E_2 trap,²² and from comparison of their relative magnitudes with the magnitudes of the signals due to the E_{2H} and E_{2L} traps in Fig. 2 we have linked the lower emission rate peak with the

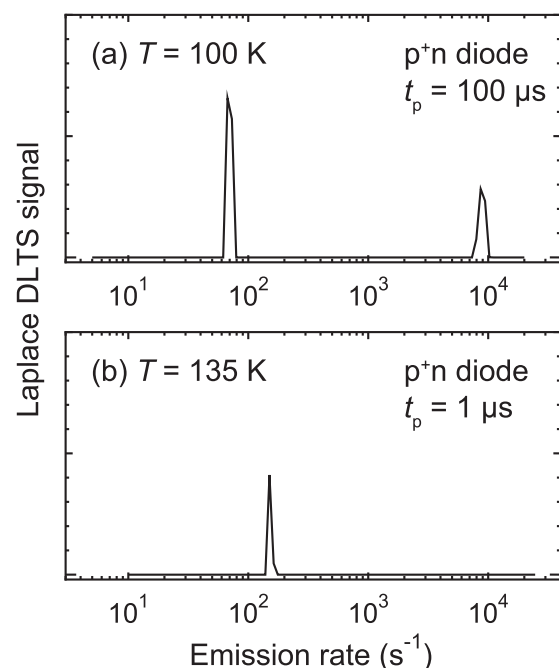


FIG. 5. LDLTS spectra at (a) 100 K and (b) 135 K recorded with filling pulse widths of $100 \mu\text{s}$ and $1 \mu\text{s}$, respectively.

TABLE I. Activation energies, pre-exponential factors, and capture cross sections of the E_1 , E_{2H} , and E_{2L} traps in n -type 6H-SiC. The capture cross-sections (σ_{na}) were calculated from the Arrhenius plots of T^2 -corrected emission rate determined from Laplace DLTS measurements.

Trap label	Deeper level			Shallower level		
	ΔE_{ne} (eV)	A_{ne} ($s^{-1} K^{-2}$)	σ_{na} (cm^2)	ΔE_{ne} (eV)	A_{ne} ($s^{-1} K^{-2}$)	σ_{na} (cm^2)
E_1	0.39	17.6	3×10^{-15}	0.26	17.3	2×10^{-15}
E_{2H}	0.43	18.0	5×10^{-15}	0.18	16.1	7×10^{-16}
E_{2L}	0.44	18.3	6×10^{-15}	0.14	15.8	5×10^{-16}

E_{2H} trap and the higher emission rate peak with the E_{2L} trap. The emission signal in the LDLTS spectra recorded in the temperature range of 130–140 K has been assigned to the shallower level of the E_1 trap. It should be mentioned that magnitudes of the LDLTS signals due to electron emission from the shallower levels, which were determined from the LDLTS measurements with a very limited number of 1 μ s filling pulses, were about half of those for their deeper counterparts. This observation further confirms the proposed links of the levels and their negative- U ordering. The activation energies for electron emission from the shallower levels of the E_1 , E_{2H} , and E_{2L} centers are found to be 0.26 eV, 0.18 eV, and 0.14 eV from the conduction band edge, respectively. The activation energies of the E_1 , E_{2H} , and E_{2L} traps as well as their pre-exponential factors and the capture cross sections calculated from the pre-exponential factors are listed in Table I. Summarizing this part of the work, we have confirmed the results of Hemmingsson *et al.*²² on the electronic structure (negative- U) of the E_1/E_2 traps. Further, the application of high resolution LDLTS enables us to resolve electron emission from the E_2 trap into two components for both the shallower and deeper levels. Both E_{2H} and E_{2L} exhibit negative- U behavior as well as E_1 .

The E_1/E_2 traps have been widely observed in the DLTS spectra of as-grown and irradiated 6H-SiC samples.^{3–10,12} The traps were attributed to the same highly abundant defect, which resides on different lattice sites in 6H-SiC.³ Although the origin of the defect is still debated,^{5,9,10} strong arguments have been presented for the assignment of the traps to energy levels of carbon vacancy (V_C).^{3,5,10} Further, according to an *ab initio* modeling study, the carbon vacancy in 4H-SiC could possess two acceptor levels with negative- U ordering in the upper half of the gap.²³ Considering similar electronic properties of defects in 4H- and 6H-SiC polytypes,¹⁴ it can be assumed that the V_C center in 6H-SiC also has an inverted order of acceptor levels. The results obtained by us are consistent with the suggested assignment of the E_1/E_2 traps in

6H-SiC to the acceptor levels of carbon vacancy. We have clearly shown that there are three components of electron emission from the deeper and shallower levels of the defect associated with the E_1/E_2 traps in 6H-SiC materials studied. These components can be attributed to the acceptor levels of the carbon vacancy at three non-equivalent lattice sites in 6H-SiC. At the three lattice sites the carbon vacancy has inverted order of the energy levels, i.e., they are all negative- U center.

This work was supported by the JSPS Institutional Program for Young Researcher Overseas Visits and in Manchester by a UK EPSRC platform grant.

- ¹H. Matsunami and T. Kimoto, *Mater. Sci. Eng. R* **20**, 125 (1997).
- ²P. J. Sellin and J. Vaitkus, *Nucl. Instrum. Methods Phys. Res. A* **557**, 479 (2006).
- ³M. O. Abouelfotoh and J. P. Doyle, *Phys. Rev. B* **59**, 10823 (1999).
- ⁴T. Dalibor, G. Pensl, H. Matsunami, T. Kimoto, W. J. Choyke, A. Schöner, and N. Nordell, *Phys. Status Solidi A* **162**, 199 (1997).
- ⁵S. Sasaki, K. Kawahara, G. Feng, G. Alfieri, and T. Kimoto, *J. Appl. Phys.* **109**, 013705 (2011).
- ⁶C. Hemmingsson, N. T. Son, O. Kordina, E. Janzén, and J. L. Lindström, *J. Appl. Phys.* **84**, 704 (1998).
- ⁷M. Gong, S. Fung, C. D. Beling, and Z. You, *J. Appl. Phys.* **85**, 7604 (1999).
- ⁸A. A. Lebedev, A. I. Veinger, D. V. Davydov, V. V. Kozlowski, N. S. Savkina, and A. M. Atrel'chuk, *J. Appl. Phys.* **88**, 6265 (2000).
- ⁹G. Pensl, T. Frank, M. Krieger, M. Laube, S. Reshanov, F. Schmid, and M. Weidner, *Physica B* **340–342**, 121 (2003).
- ¹⁰X. D. Chen, C. L. Yang, M. Gong, W. K. Ge, S. Fung, C. D. Beling, J. N. Wang, M. K. Lui, and C. C. Ling, *Phys. Rev. Lett.* **92**, 125504 (2004).
- ¹¹K. Dmowski, *Rev. Sci. Instrum.* **61**, 1319 (1990).
- ¹²G. Pensl and W. J. Choyke, *Physica B* **185**, 264 (1993).
- ¹³L. Patrick, *Phys. Rev. B* **5**, 2198 (1972).
- ¹⁴E. Janzén, A. Gali, A. Henry, I. G. Ivanov, B. Magnusson, and N. T. Son, in *Defects in Microelectronic Materials and Devices*, edited by D. M. Fleetwod, S. T. Pantelides, and R. D. Schrimpf (CRS, Boca Raton, 2009), p. 615.
- ¹⁵L. Dobaczewski, A. R. Peaker, and K. B. Nielsen, *J. Appl. Phys.* **96**, 4689 (2004).
- ¹⁶N. Iwamoto, S. Onoda, T. Makino, T. Ohshima, K. Kojima, A. Koizumi, K. Uchida, and S. Nozaki, *IEEE Trans. Nucl. Sci.* **58**, 305 (2011).
- ¹⁷T. Kimoto, A. Itho, and H. Matsunami, *Phys. Status Solidi B* **202**, 247 (1997).
- ¹⁸A. A. Rempel, W. Sprengel, K. Blaurock, K. J. Reichle, J. Major, and H. E. Schaefer, *Phys. Rev. Lett.* **89**, 185501 (2002).
- ¹⁹L. Storasta, J. P. Bergman, E. Janzén, A. Henry, and J. Lu, *J. Appl. Phys.* **96**, 4909 (2004).
- ²⁰A. Uedono, T. Ohshima, H. Itoh, R. Suzuki, T. Ohdaira, S. Tanigawa, Y. Aoki, M. Yoshikawa, and T. Mikado, *Jpn. J. Appl. Phys.* **37**, 2422 (1998).
- ²¹A. Uedono, S. Tanigawa, T. Ohshima, H. Itoh, M. Yoshikawa, I. Nashiyama, T. Frank, G. Pensl, R. Suzuki, T. Ohdaira, and T. Mikado, *J. Appl. Phys.* **87**, 4119 (2000).
- ²²C. G. Hemmingsson, N. T. Son, and E. Janzén, *Appl. Phys. Lett.* **74**, 839 (1999).
- ²³A. Zywiets, J. Furthmüller, and F. Bechstedt, *Phys. Rev. B* **59**, 15166 (1999).